

Anisotropy of the physisorption interaction between H₂ and metal surfaces

L. Wilzén, F. Althoff, and S. Andersson

Department of Physics, Chalmers University of Technology, S-412 96 Göteborg, Sweden

M. Persson

Institute of Theoretical Physics, Chalmers University of Technology, S-412 96 Göteborg, Sweden

(Received 9 July 1990)

The orientational dependence of molecule-surface interaction has been studied both experimentally and theoretically. Rotational substrate splittings of corrugation-mediated selective adsorption resonances observed for H₂ molecular beams scattered from a Cu(100) surface are compared with predictions from the standard theory of physisorption. We find that the measured anisotropy is dominated by the van der Waals interaction and that the repulsive contribution is much smaller than anticipated. We show that an extension of the theory that includes interaction of the metal electron states with the antibonding resonance of H₂ strongly reduces the repulsive anisotropy and brings theory into agreement with experiment.

I. INTRODUCTION

The physisorption interaction of a gas-phase particle with a solid surface is thought to be, to a very good approximation, electronically adiabatic. The energy transfer then takes place through the phonon system of the solid lattice. These conditions are believed to hold for the light rare gases adsorbing on all solids and for H₂ on simple and noble metals.

In the molecular case, rotational and vibrational inelastic collisions may also be involved in the energy transfer. The vibrational excitation energies for H₂ and D₂ are high, the $\nu=0 \rightarrow 1$ lie at 516 and 371 meV for H₂ and D₂, respectively, and will be of no importance in the scattering of thermal low-energy molecular beams in the range 10–100 meV. These excitations may be importantly involved at higher beam temperatures and energies, e.g., in the activated dissociation of H₂ on copper surfaces.^{1–3} The rotational excitations will be of importance, however, since the energies are in the energy range of concern, e.g., the $J=0 \rightarrow 2$ transitions lie at 44 and 22 meV for H₂ and D₂, respectively.

The occurrence of rotational transitions in the scattering of H₂ and D₂ molecular beams from solid surfaces is well documented in the literature. They give rise to, e.g., coherent inelastic diffraction events in the angular distribution of scattered particles.⁴ Rotational transitions to the bound-state levels of the physisorption potential will cause rotationally mediated selective adsorption (RMSA) resonances in the angular dependence of the elastic specular scattering intensity.⁵ Combined resonances involving both rotational excitation and diffraction, corrugation-rotation-mediated selective adsorption (CRMSA), have been observed in both scattering and sticking of H₂ and D₂ on Cu(100).⁶

The probability for rotational transitions is related to the angular dependence of the H₂-surface interaction, and

the measurement of rotationally inelastic transition probabilities can thus give information about the anisotropy of the interaction. Corrugation-mediated selective adsorption (CMSA) resonances provide another way to study the anisotropy. These resonances derive from diffraction events that trap the incident particle into bound-state levels of the physisorption well. Owing to the anisotropy of the interaction these resonances depend on the molecular rotational state. The $(2J+1)$ -fold degeneracy within a given rotational multiplet will be lifted. In a nice beam scattering experiment, Chiesa *et al.*⁷ managed to resolve the J -dependent splitting of CMSA resonances observed for H₂ scattered from an Ag(110) surface. They established their interpretation by comparing resonance data for n -H₂ and p -H₂ beams. The normal-hydrogen n -H₂ beam has a thermal rotational population (ratio of even J to odd J is 1 to 3) of predominantly $J=0$ and 1 molecules and the parahydrogen p -H₂ beam is composed solely of even- J molecules, mostly $J=0$. The experimental observations were analyzed theoretically by Schinke, Engel, and Voges⁸ within the standard theory of physisorption, which states that the laterally averaged anisotropic part $V_2(Z)$ of the physisorption potential can be written as a linear combination of the repulsive and attractive parts V_R and V_{VW} of the laterally averaged isotropic potential, i.e., $V_2(Z) = \beta_R V_R(Z) + \beta_{VW} V_{VW}(Z)$. Harris and Feibelman have shown that the anisotropy of the polarizability tensor of the free H₂ molecule gives $\beta_{VW} = 0.05$.⁹ This asymmetry of the van der Waals interaction favors rotations about axes parallel to the surface, i.e., $M=0$. The magnitude of the observed resonance splittings for H₂ scattered from Ag(110) was found to be well fitted for $\beta_R = 0.2$ adopting $\beta_{VW} = 0.05$.⁸ This picture is also supported by theoretical calculations of the repulsive part,¹⁰ which dominates the anisotropic interaction and favors rotations about axes normal to the surface, i.e., $M=J$.¹¹

Contrasting these results Whaley *et al.*¹² did not ob-

serve any distinct splitting of CMSA resonances observed for H_2 scattering from Ag(111). They observed a broadening of the n - H_2 data as compared to those obtained using p - H_2 beams. Analysis of these data gave an anisotropic potential with $\beta_R=0.10$ and $\beta_{vw}=0.06$. *A priori* it is somewhat difficult to understand this difference in the physisorption interaction of H_2 with two different Ag surfaces that otherwise give a very similar laterally averaged isotropic potential. Theoretical estimates do not suggest any significant difference.¹⁰

In a series of scattering and sticking investigations of H_2 on Cu(100) we noted⁶ that structure due to RMSA resonances tended to be weaker than expected while the combined CRMSA resonances were stronger than expected. This conclusion was based on a comparison of experimental data with theoretical estimates using the anisotropic interaction discussed above. We felt urged to investigate this problem in further detail.

In this paper we will describe experiments that measure the splitting of CMSA resonances observed for n - H_2 scattered from Cu(100). We find that the magnitude of the splitting is very similar to that observed for the Ag(110) surface. We determine the sign of the splitting, both from the relative intensity of the resonances and the relative position in energy of the n - H_2 resonances and the corresponding p - H_2 resonance. We find, to our surprise, that the sign is reversed compared to the value adopted for Ag(110). The laterally averaged isotropic potential for Cu(100) is very similar to that for Ag(110) (Ref. 13) and we would also expect the anisotropy to be rather similar. The reversed sign is compatible with a small value of $\beta_R = -0.002$, i.e., the anisotropy is dominated by the van der Waals term with $\beta_{vw}=0.05$.

In this context we note that Schinke, Engel, and Voges⁸ found that they could reproduce the magnitude of the resonance splitting observed for n - H_2 scattering from Ag(110) using $\beta_R=0.01$. This small β_R value is in fact compatible with the experimentally suggested ordering of the (J,M) sublevels.⁷ Schinke *et al.* argued, however, that the sign of the splittings could not be determined and that this low β_R value was unphysical, while the larger β_R value compares favorably with theoretical estimates. On the basis of our results for H_2 -Cu(100), we are convinced that the experimentally suggested interpretation of the H_2 -Ag(110) data is the correct one and that the two systems display similar anisotropic interaction.

Our observations reveal a striking disagreement between theory and experiment, which suggests that either the theory is not able to describe this detail of the interaction or that the particular approach used in the calculations misses an important ingredient of the anisotropy. We present evidence that the latter is the case. The calculations neglect the anisotropic interaction with the antibonding σ_u resonance of H_2 . We estimate from a simple model calculation that this contribution is strong enough to almost cancel the anisotropy due to the bonding σ_g state of H_2 . We do not exclude that other effects may be involved, but we do believe that the anisotropic interaction with the σ_u resonance is the primary correction to the calculational approach.

II. EXPERIMENTAL

In this section we describe experiments that measure the rotational anisotropy of H_2 molecules interacting with the clean Cu(100) surface. The apparatus used consisted of a molecular-beam stage, a scattering chamber, control electronics, and a data acquisition system. H_2 nozzle beams were shaped by skimmers in three turbopumped chambers. The gas was expanded from a 10- μ m-diam nozzle source at temperatures between 30 and 300 K combining cooling by helium gas transferred from a liquid-helium Dewar and resistive heating. This technique enabled us to keep the source temperature stable to ~ 0.1 K. The hydrogen gas was precooled to liquid-nitrogen temperature before entering the nozzle source. The source temperature was controlled electronically via a thermocouple (Au 0.03% Fe-Cromel) signal and could be kept steady, ramped stepwise, or linearly in time. Hydrogen pressures around 1 bar produced adequate molecular beams over the entire source temperature range with an optimum energy spread of 10%. The beam angular divergence was 0.29° . The resonance measurements were made with n - H_2 beams having thermal rotational populations (ratio of even J to odd J is 1 to 3) and p - H_2 beams composed solely of even- J rotational states. These beams were produced via on-line conversion of the normal gas by use of a nickel silicate catalyst kept at 25 K by a cool helium-gas flow.

The scattering experiments were carried out in a cryopumped (1000 l/s) ultrahigh vacuum chamber operating at a base pressure of 3.10^{-11} Torr. The chamber pressure increased to typically 5×10^{-10} Torr with the molecular beam on and pressure oscillations were negligible. Incident and scattered beam intensities were measured using a rotatable stagnation detector with an angular resolution of 1.5° . The detector, constructed from oxygen-free high-conductivity copper to minimize outgassing and charging up effects, was equipped with a calibrated ionization gauge and mounted on a bellows construction enabling movement by 80° in the scattering plane and $\pm 25^\circ$ normal to the scattering plane. A separate copper valve on the detector body allowed proper outgassing of the ionization gauge. The latter was equipped with a low-temperature filament in order to minimize any influence on thermal dissociation on the pressure readings. The pressure signal was read by an electrometer directly attached to the gauge-detector construction. This arrangement minimized microphonic noise when the detector was moved. The signal was read in dc mode since the chamber pressure was very stable. Beam energies and the relative rotational populations of normal and converted H_2 beams were obtained by performing diffraction measurements using the same detection arrangement.

The Cu(100) specimen was spark-cut from a 5-N purity Cu single crystal rod and oriented by x-ray back diffraction to about 0.1° to ensure a low step density. The sample was subsequently mechanically and electrolytically polished to optical flatness and finish and mounted in the scattering chamber. The surface was cleaned *in situ* by standard methods involving argon-ion bombardment

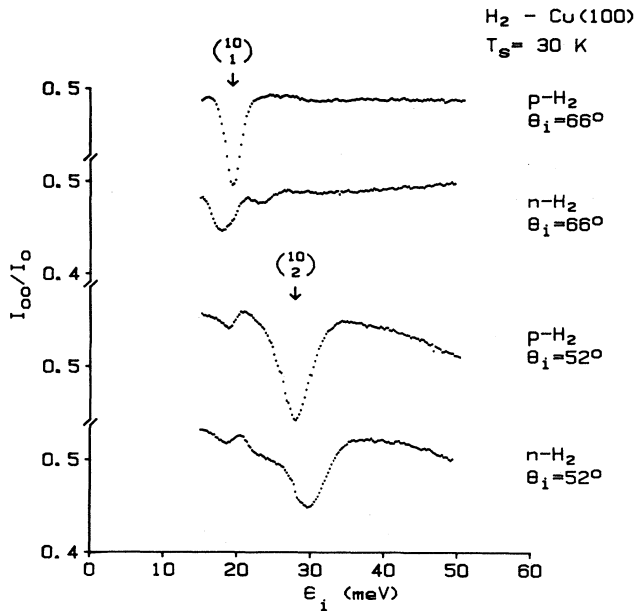


FIG. 1. Corrugation-mediated selective adsorption (CMSA) resonances in the specular beam of p -H₂ and n -H₂. The resonance dips in the measured intensity I_{00}/I_0 of the specular beam due to the bound states $n=1$ and 2 are shown as a function of incident energy E_i for two different angles of incidence θ_i and are labeled by (10_1) and (10_2) , respectively.

and heating cycles. It could be cooled to ~ 10 K using cool helium gas transferred from a liquid-helium Dewar as cryoagent and was heated resistively using an electronically controlled power supply. The Cu(100) specimen was mounted with respect to the direction of the incident molecular beam so that the scattering plane comprised the surface normal and the [010] direction in the surface plane. The accuracy of this alignment was better than 0.2° as determined by diffraction measurements around the scattering plane.

In the resonance measurements discussed below, the specular beam intensity I_{00} , incident beam intensity I_0 , and nozzle source temperature T_N were sampled, normalized, and plotted using a Hewlett-Packard HP200 series microcomputer and a HP7090A measurement plotting system. The Cu(100) specimen was kept at 30 K during the intensity versus T_N scans and was cleaned by flash heating to 900 K between each measurement. A more detailed description of the apparatus and the experimental procedure has been presented previously.⁶

Figure 1 displays typical experimental specular reflectivity data I_{00}/I_0 obtained for n -H₂ and p -H₂ beams scattered from the Cu(100) specimen. For a given angle of incidence all the angular settings of the instrument were kept fixed and only the gas was changed from n -H₂ to p -H₂. This precaution was important since these resonances disperse very quickly with incident angle θ_i . The incident n -H₂ and p -H₂ beam intensities were measured when the specular reflectivity measurements for a series of θ_i values were completed. The prominent reflectivity

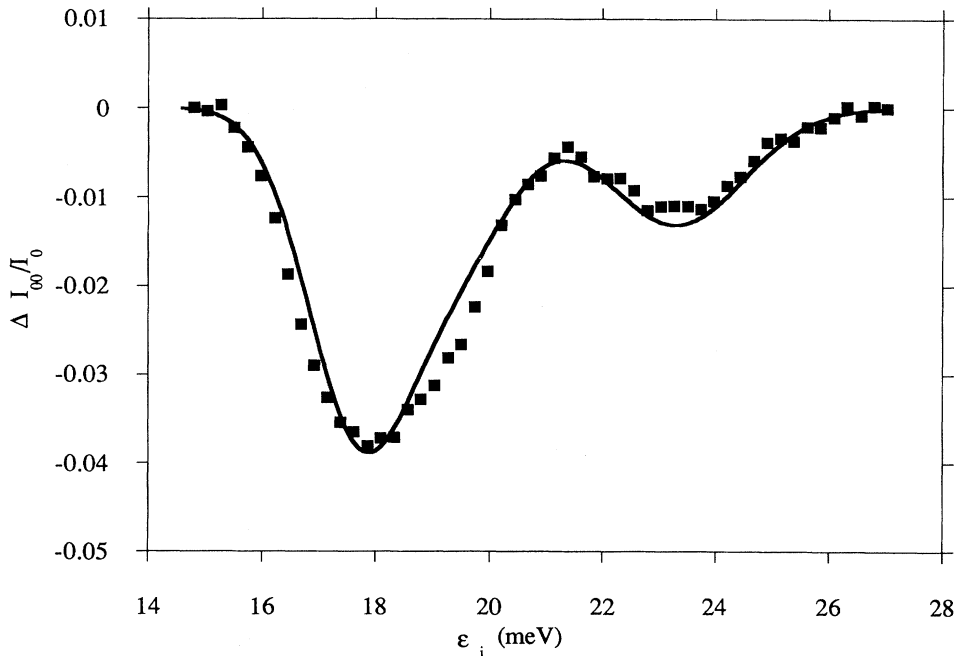


FIG. 2. Simulated fit (solid curve) to the experimental specular resonance data for n -H₂ at $\theta_i = 66^\circ$ (squares). A smooth background has been subtracted from the experimental specular reflectivity curve. See text for details about the fitting procedure.

dips in the p -H₂ curves at $\theta_i = 66^\circ$ and 52° are associated with corrugation-mediated selective adsorption resonances involving the first-order reciprocal lattice vector \mathbf{G}_{10} and the bound state levels $n = 1$ and 2 of the H₂-Cu(100) physisorption potential. These resonances are denoted as $(\begin{smallmatrix} 10 \\ 1 \end{smallmatrix})$ and $(\begin{smallmatrix} 10 \\ 2 \end{smallmatrix})$ in Fig. 1. Since these resonances are observed using p -H₂ beams at low nozzle temperatures, we know that the molecular rotational state is predominantly $(J, M) = (0, 0)$. The weaker minimum around 20 meV, in the $\theta_i = 52^\circ$, p -H₂ reflectivity curve, derives from a higher-order diffraction event identified as $(\begin{smallmatrix} 11 \\ 3 \end{smallmatrix})$.

The $(\begin{smallmatrix} 10 \\ 1 \end{smallmatrix})$ and $(\begin{smallmatrix} 10 \\ 2 \end{smallmatrix})$ resonances show up as two resolved minima in the n -H₂ reflectivity curves. This splitting is evidently related to the rotational distribution of the n -H₂ gas. We have analyzed these data, as is shown in Fig. 2, by means of a computed simulation (solid curve) that mimics the experimental data (squares) in this case n -H₂, $\theta_i = 66^\circ$. The resonance linewidths and the energy of the $(J, M) = (0, 0)$ resonance used in the simulation were obtained from the corresponding p -H₂ measurement. The relative spectral weights of the $(J, M) = (0, 0)$, $(1, \pm 1)$, and $(1, 0)$ states were taken to be $\frac{1}{4}$, $\frac{2}{4}$, and $\frac{1}{4}$, respectively, while the energies of the $(1, \pm 1)$ and $(1, 0)$ resonances were adjusted so that the simulation fitted the experimental data. The weaker minimum is related to the $(J, M) = (1, 0)$ resonance, while the stronger one is dominated by the $(1, \pm 1)$ resonance. In this way the resonance energies were determined for several angles of incidence as displayed in Fig. 3. The solid curves correspond to free-particle dispersion curves fitted by a least-squares method to the experimental resonance energies. The

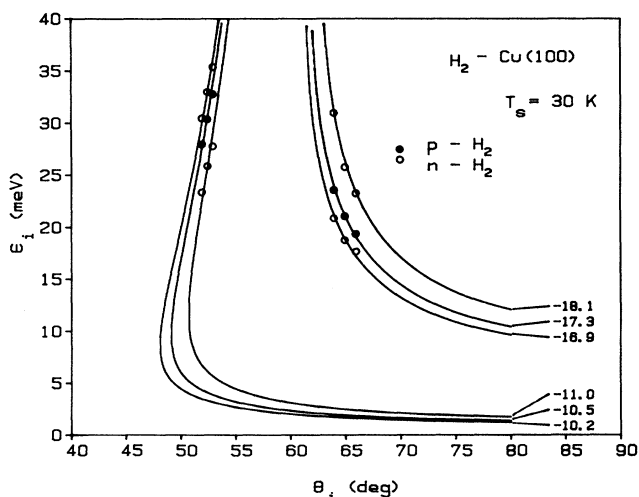


FIG. 3. Dispersion of the rotational substates of the CMSA resonances of p -H₂ and n -H₂. The open (n -H₂) and solid circles (p -H₂) are the measured energies ε_i of the resonance dips as a function of the incident angle θ_i . The depicted bound-state energies are determined kinematically by assuming free-particle dispersion along the surface for the adsorbed particles (solid lines).

$(J, M) = (1, 0)$ state corresponds to the lowest lying level at $\varepsilon_1 = -18.1$ meV and $\varepsilon_2 = -11.0$ meV. The ratio of the $(J, M) = (1, 0)$ and $(1, \pm 1)$ shifts with respect to the $(J, M) = (0, 0)$ isotropic case is -2.0 and -1.7 for the $(\begin{smallmatrix} 10 \\ 1 \end{smallmatrix})$ and $(\begin{smallmatrix} 10 \\ 2 \end{smallmatrix})$ resonances. This is in satisfactory agreement with the ratio -2 found from first-order perturbation theory, considering that the uncertainties in the determination of the resonance energies is larger for $(\begin{smallmatrix} 10 \\ 2 \end{smallmatrix})$ resonance.

III. ANALYSIS OF EXPERIMENTAL DATA

The observed J -dependent splitting of a CMSA resonance shows directly that the molecule-surface interaction energy depends on the orientation of the molecule with respect to the surface normal. For instance, in the case of the rotational ground state of o -H₂, $J = 1$, the state with $M = 0$ tends to have its molecular axis in the normal direction, whereas the states with $M = \pm 1$ tend to have their axis parallel to the surface. An angular dependence of the molecule-surface interaction energy will thus shift the energies of these substates differently. The small splitting of the observed CMSA resonances compared to the level spacing shows that the anisotropic part of the interaction potential is weak compared to the isotropic part and may be analyzed using perturbation theory.

The anisotropic component of the laterally averaged interaction potential will give rise to a first-order splitting of the rotational sublevels. This component is identified by an expansion of the laterally averaged potential in Legendre functions as

$$V(Z, \theta) = \sum_{l=0}^{\infty} V_l(Z) P_l(\cos \theta). \quad (1)$$

Here Z is the distance of the center of mass of the molecule from the surface and θ is the polar angle between the molecule axis and the surface normal. Note that no dependence on the azimuthal angle is introduced by the laterally averaged potential and that the sum over l in Eq. (1) is restricted to even integers for a homonuclear molecule like hydrogen. The weakness of the anisotropic interaction suggests that the anisotropy is dominated by the $l = 2$ term $V_2(Z)$.

The term $V_2(Z)$ shifts the energies of the rotational substates (J, M) of a molecule in a bound state level n ,⁹

$$\Delta E_n^{(J, M)} = \frac{3 \langle n | V_2 | n \rangle}{(2J+3)} \left[\frac{J^2 - M^2}{2J-1} - \frac{J}{3} \right], \quad (2)$$

where $\langle n | V_2 | n \rangle$ is the matrix element of $V_2(Z)$ with respect to the bound-state wave function of level n . The shift of the rotational ground state of p -H₂, $J = 0$ is zero due to the isotropic distribution of the molecular axis for this state. The shifts of the sublevels of the rotational ground state of o -H₂, $J = 1$ satisfies, independently of the level n , the simple relation $\Delta E_n^{(1, 0)} : \Delta E_n^{(1, \pm 1)} = 2 : -1$. The observed splittings of the CMSA resonances in Fig. 3 are well satisfied by this relation. The observed resonance intensity (see Fig. 2) of the least shifted, doubly degenerate, substates, $M = \pm 1$, is approximately twice as large as the

intensity of the most shifted singlet, $M=0$, in accordance with expectation. Hence it is straightforward to make an assignment of the azimuthal quantum numbers to the observed levels. In particular, this assignment shows that $\langle n|V_2|n\rangle$ is negative for $n=1,2$, which amounts to the fact that the rotational anisotropy favors the molecule to be oriented normal to the surface.

The magnitudes of $\langle n|V_2|n\rangle$ for $n=1,2$ are extracted from the observed energy splittings $E_n^{(1,0)} - E_n^{(1,\pm 1)}$ using Eq. (2) and are presented in Fig. 4. The splitting of the rotational substates of the $(\frac{10}{3})$ resonance has not been resolved, but appears as an extra broadening of the resonance line. Instead we have extracted the magnitude of the splitting indirectly by simulating the observed line shape. This simulation amounts to a forward convolution of a Gaussian mimicking the energy resolution, a half-circle representing the angular divergence of the incident molecular beam, and a Lorentzian representing the intrinsic broadening. The magnitude of the latter is determined from the analysis of the line shape due to the $p\text{-H}_2$ beam. The resulting $\langle 3|V_2|3\rangle$ is also presented in Fig. 3.

We now turn to a comparison of measured splittings with the results from the standard theory of physisorption. First we have to discuss the isotropic component of

the laterally averaged interaction potential V_0 in order to determine the bound states $|n\rangle$ appearing in the matrix element $\langle n|V_2|n\rangle$.

In the standard theory of physisorption, the molecule-surface interaction is decomposed into a van der Waals attraction and a Pauli repulsion introduced by the overlap of the electron densities of the metal and the molecule. These two terms contribute additively to the laterally averaged isotropic interaction potential as

$$V_0(Z) = V_R(Z) + V_{\text{VW}}(Z), \quad (3)$$

where

$$V_R(Z) = V_0 \exp(-\alpha Z), \quad (4)$$

and

$$V_{\text{VW}}(Z) = C_{\text{VW}} \frac{f_2[2k_c(Z - Z_{\text{VW}})]}{(Z - Z_{\text{VW}})^3}. \quad (5)$$

Here V_0 and α determine the strength and inverse range of the repulsive potential, respectively, C_{VW} is the strength of the asymptotic van der Waals attraction, and Z_{VW} is the position of the van der Waals plane for the metal. The saturation of the attraction due to the finite size of the molecule is given by the cutoff function

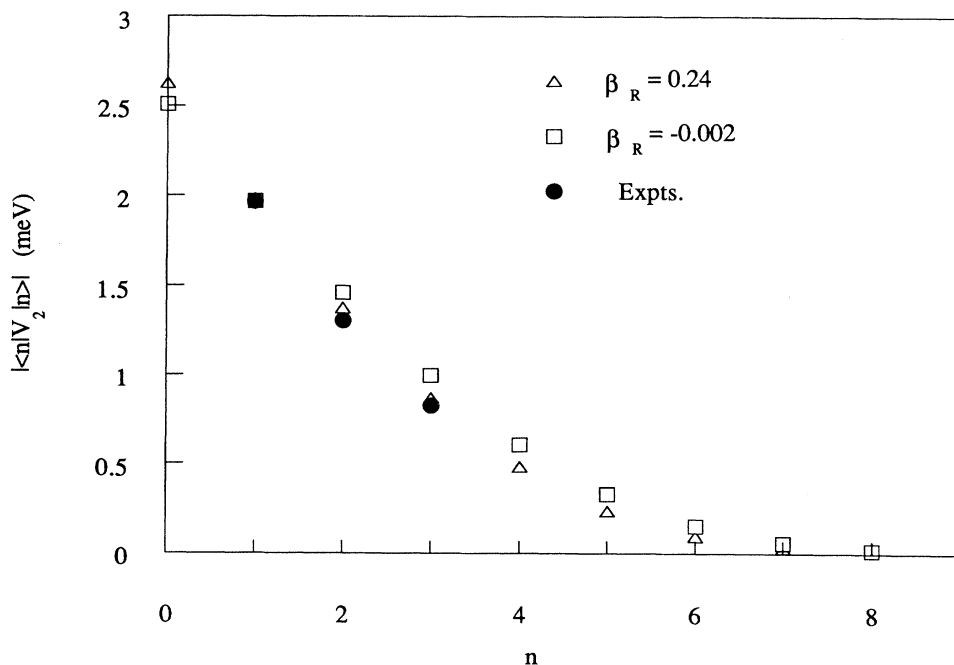


FIG. 4. Comparison between calculated and experimental $|\langle n|V_2|n\rangle|$. The solid circles are the measured absolute magnitude of the splittings $|\langle n|V_2|n\rangle|$ as a function of the bound-state level n . The open triangles and squares are the calculated $|\langle n|V_2|n\rangle|$ for two different values β_R of the anisotropy parameter of the repulsive part of the interaction potential that fits the experimental data. The value $\beta_R=0.24$ is close to the calculated value of 0.18 in the standard theory of the physisorption, but gives the wrong sign for $\langle n|V_2|n\rangle$ (Ref. 10). The smaller value $\beta_R=-0.002$ gives good agreement both with respect to absolute magnitude and sign of $\langle n|V_2|n\rangle$.

$f_2(x) = 1 - (1 + x + x^2/2)\exp(-x)$, where k_c is related to the inverse size of the molecule.¹⁰

The trends for the binding energies over different physisorbates are well reproduced by this theory, but the agreement is worse on trends over different metal surfaces. For instance, the observed binding energy of H_2 on Cu(100) (Ref. 13) is underestimated by about 9 meV, whereas for Ag the agreement is excellent. This disagreement is not necessarily a failure of the theory since the present uncertainties in C_{VW} can give rise to this difference in binding energy due to the delicate balance between V_R and V_{VW} . By a slight tuning of these parameters, this exp-3 potential is able to reproduce the positions of the bound-state levels as deduced from measurements of the dispersion of CMSA resonances both for H_2 and D_2 on Cu(100).¹³ This good agreement, as shown in Table I, demonstrates that the functional form given in Eqs. (4) and (5) is an accurate description of $V_0(Z)$.

The standard theory of physisorption also gives the laterally averaged anisotropic component $V_2(Z)$ as a linear combination of the repulsive and attractive parts of V_0 , Eqs. (4) and (5),

$$V_2(Z) = \beta_R V_R(Z) + \beta_{VW} V_{VW}(Z). \quad (6)$$

The anisotropy of the polarizability tensor of the free H_2 molecule gives $\beta_{VW} = 0.05$ on Cu(100),⁹ a value that is going to be used throughout our discussion for this system.

Calculations of the anisotropy of the repulsive part give $\beta_R = 0.18$.¹⁰ The magnitude of the observed splittings of the bound-state levels of H_2 on Ag(110) are well reproduced by a minor tuning of β_R to 0.2 (Ref. 8) from the calculated value $\beta_R = 0.17$.¹⁰ Note that on this surface the calculated value $\beta_{VW} = 0.05$ is also close to the corresponding value on Cu(100). As shown in Fig. 4 the magnitude of the observed splittings on Cu(100) are also reproduced by $\beta_R = 0.24$, i.e., close to the calculated value. In their analysis of the observed splittings on Ag(110), Schinke, Engel, and Voges⁸ noted that a value of $\beta_R = 0.01$ also reproduces the magnitude of the splittings. They argue, however, that the experiments could not determine the sign of the splittings, i.e., the sign of $\langle n | V_2 | n \rangle$ in Eq. (2), and that the low value is unphysical and accordingly suggested the larger value for β_R .

We have demonstrated from the observed intensities and ratio of the shifts of the rotational substates of the CMSA resonances that it is possible to determine the sign of $\langle n | V_2 | n \rangle$. We find that both the magnitude and sign of the observed splittings are only reproduced by a low value for β_R of -0.002 . We note that a small β_R value is also compatible with the experimentally suggested ordering of the (J, M) sublevels for the H_2 -Ag(110) system.⁷ This lower value means that $\langle n | V_2 | n \rangle$ is negative, which favors a molecular orientation with the axis normal to the surface in contrast to the theoretical result, that $\langle n | V_2 | n \rangle$ should be positive, which would favor a paral-

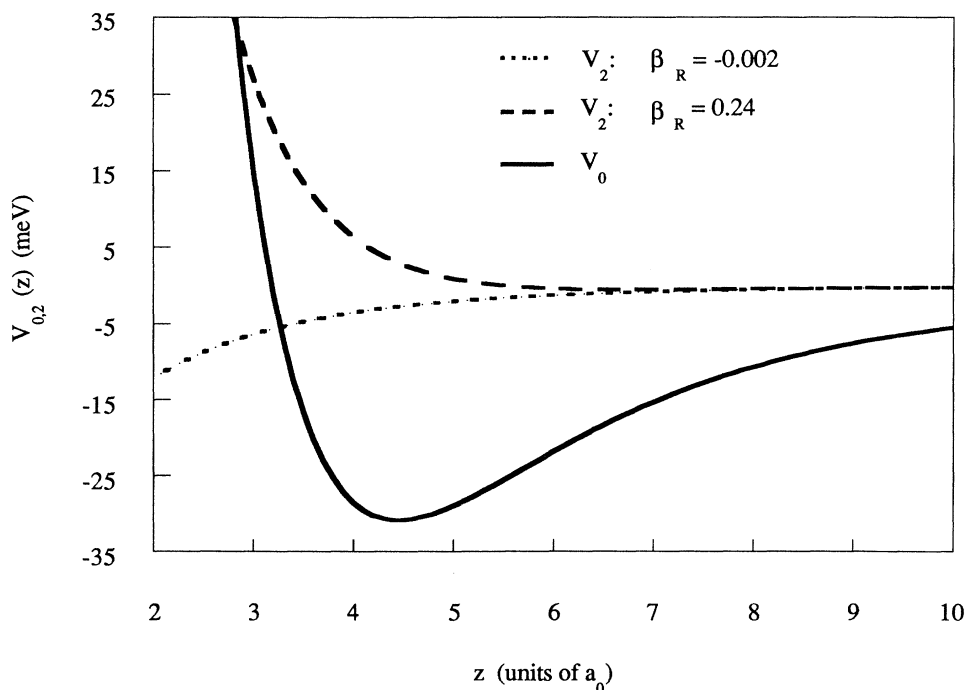


FIG. 5. Models for the anisotropic potential V_2 . The two different models for V_2 with parameters β_R that fit the absolute magnitude of the measured splittings $|\langle n | V_2 | n \rangle|$ are shown as a function of the distance z from the jellium edge. Their magnitudes are compared with the physisorption potential V_0 . Note that the model that gives the correct sign for $\langle n | V_2 | n \rangle$ corresponding to $\beta_R = -0.002$ is dominated by the anisotropy of the attractive part of V_0 .

TABLE I. Experimental and calculated bound-state levels. The bound-state levels have been calculated numerically from the exp-3 potential, Eqs. (4) and (5), using the parameters $V_0 = 5.21$ eV, $\alpha = 1.21a_0^{-1}$, $C_{vw} = 4.74$ eV a_0^{-3} , $Z_{vw} = 0.563a_0$, $k_c = 0.45a_0^{-1}$ with the origin at the jellium edge.

n	$-E_n$ (meV)	
	(p-H ₂)	(exp-3)
0	25.7	25.54
1	17.3	16.66
2	10.5	10.07
3	5.7	5.54

lel orientation. This disagreement between theory and experiment suggests that either the theory is not able to describe this detail of the interaction or the pseudopotential expansion used in the calculation misses an important ingredient of the anisotropy. Later on we will present evidence that this expansion is not able to describe the interaction with the antibonding resonance of the hydrogen molecule. It turns out, from a simple model calculation, that this term is able to almost cancel the anisotropy due to the bonding state of H₂.

While the magnitudes of the splittings of the rotational sublevels are about the same for the two different choices of β_R , they give dramatically different strengths for rotational transitions as in rotationally inelastic scattering and rotationally mediated selective adsorption resonances. This effect is already evident from Fig. 5, where these two different forms for V_2 are compared. The new form of $V_2(Z)$ has a much smaller variation with Z around the backwall of $V_0(Z)$ than the form suggested by $\beta_R = 0.24$ and should give much smaller matrix elements for transitions between states with different energies E_{\perp} of the motion normal to the surface.

This new different spatial behavior of $V_2(Z)$ explains a puzzling feature of the specular scattering experiments of H₂ and D₂ from Cu(100), namely that no RMSA resonance has been observed while the theoretical value $\beta_R = 0.18$ gives partial widths for the RMSA resonances that are of the same order as for the observed CMSA resonances. The calculated partial widths at normal incidence condition given in Table II show that the value for $\beta_R = -0.002$ extracted from the measured splittings

TABLE II. Calculated partial widths of rotationally mediated selective adsorption (RMSA) resonances.

$\left[\begin{array}{c} 0 \rightarrow 2 \\ n \\ n \end{array} \right]$	Γ_i (μ eV)	
	$\beta_R = 0.24$	$\beta_R = -0.002$
0	27	0.3
1	49	0.5
2	55	0.6
3	47	0.5
4	31	0.3

decreases these partial widths with several orders of magnitudes and explains why these resonances are not observed. The partial widths were calculated using a method based on close-coupled channels. The strength of rotationally inelastic scattering has been analyzed for H₂ from Ag(111).¹² The intensity of the measured $j \rightarrow j' = 0 \rightarrow 2$ peak was reproduced by a value of $\beta_R = 0.09$, correcting for phonon inelasticity by a phenomenological Debye-Waller factor. The similar behavior of the physisorption interaction of H₂ with Cu and Ag, and in particular the similar anisotropic interaction of H₂ with Cu(100) and Ag(110), suggests a value of $\beta_R = 0.0$. This value gives about a factor of 2 small intensity. Considering the uncertainties in their Debye-Waller correction procedure, we argue that this agreement is acceptable, while a value of $\beta_R = 0.2$ gives a too large intensity by factor of 5.

IV. THEORY OF ANISOTROPIC POTENTIAL

In this section we identify an important contribution to the anisotropic molecule-metal interaction that is not accounted for in the earlier calculations based on the standard theory for physisorption. This new term derives from the interaction of metal electron states with the antibonding resonance σ_u of the molecule. This interaction is expected to be strongly anisotropic due to the p_z symmetry of σ_u with respect to the molecular axis. We present a simple electronic structure model which shows that the anisotropy of the repulsive barrier is more or less canceled by this interaction.¹⁴

The standard theory of physisorption is based on an approximate treatment of the molecule-metal exchange-correlation energy. Terms in the correlation energy of first order in the overlap between the metal and molecule wave functions are neglected. The van der Waals attraction is due to the correlation between the motion of the metal conduction electrons and the electrons in the σ_g molecular orbital and is of zero order effect in this overlap. The repulsive part of the interaction is of first order in the overlap and is given in terms of one-electron energy shifts $\delta\epsilon_m = \epsilon_m - \epsilon_m^0$ of the occupied metal states as^{15,16}

$$V_R(Z, \theta) = 2 \sum_{occ m} \delta\epsilon_m, \quad (7)$$

where the factor of 2 accounts for the spin degeneracy. The energy ϵ_m^0 is determined from the one-electron potential of the bare model v_{met} .

In the case of the helium-metal surface interaction a calculational method based on a perturbation expansion in the atomic pseudopotential has been shown to give a good result for the one-electron energy sum (7), in comparison with the result from a full scattering calculation.¹⁷ The main justification for its use in the case of the hydrogen-metal surface interaction is based on the fact that the second-order term in the pseudopotential expansion is found to be only 25% of the first-order term.¹⁰ This second-order term is calculated using a spherically averaged pseudopotential and gives accordingly no contribution to the rotational anisotropy. A perturbative ex-

pansion, however, in terms of the full pseudopotential over the bare metal states, is not able to include properly the interaction with a resonant state like σ_u of hydrogen. Instead we are going to introduce the effects of the resonance explicitly by considering a simple three-level model.

The three-level system comprises an occupied single level $|m\rangle$ representing a metal state, and an occupied level $|g\rangle$ and an unoccupied level $|u\rangle$, representing the bonding state σ_g and the antibonding resonance state σ_u of the molecule, respectively. The leading-order contribution in the shift $\delta\epsilon_m$ of the metal state in terms of the overlaps $\langle g|m\rangle$ and $\langle u|m\rangle$ can be written as a sum of the individual shifts $\delta\epsilon_m^g$ and $\delta\epsilon_m^u$ due to the interaction with $|g\rangle$ and $|u\rangle$, respectively. Neglecting the variation of v_{met} over the molecule, as done in the derivation of the pseudopotential expansion, brings the shift $\delta\epsilon_m^g$ to the same form as the first-order term in this expansion,

$$\delta\epsilon_m^g = \langle m|v_{\text{mol}}|m\rangle + [\epsilon_m^0 - \epsilon_g^0 - v_{\text{met}}(\mathbf{Z})] |\langle g|m\rangle|^2. \quad (8)$$

Here ϵ_g^0 is the one-electron energy of the ground-state orbital $|g\rangle$ of the free molecule. The first term gives the energy gain in the attractive H_2 potential, which is balanced by the second repulsive term due to the orthogonalization against σ_g . The shift $\delta\epsilon_m^u$ from the interaction with the unoccupied $|u\rangle$ can be reduced to a second-order perturbation expression,

$$\delta\epsilon_m^u = - \frac{|\langle m|v_{\text{mol}}|u\rangle|^2}{\epsilon_u^0 - \epsilon_m^0}, \quad (9)$$

where ϵ_u^0 is the one-electron energy of the antibonding orbital of the free molecule. This term gives the energy gain from the virtual transition of the metal electron to the unoccupied molecular state. Note that the corresponding second-order term in the pseudopotential expansion involves a sum over unoccupied metal states, while Eq. (9) contains only one intermediate state representing the antibonding molecular resonance.

In order to obtain a quantitative estimate of the anisotropy within this three-level model and also to make contact with previous calculations by Nordlander, Holmberg, and Harris,¹⁰ we have used their specific model for the metal and molecule states. The details of this model and the calculations based on a Monte Carlo integration method are both described in the Appendix. We have calculated $\delta\epsilon_m$ at the equilibrium distance of the molecule, $\mathbf{Z} = \mathbf{Z}_{\text{eq}}$, for a few representative metal states: one state with a normal energy $\epsilon_{\perp} = \epsilon_F$ and two states with normal energies in the region of 1–2 eV below ϵ_F where the sum (7) gets its dominant contribution. The isotropic component of $\delta\epsilon_m^u$ is found to be small compared to the corresponding component of $\delta\epsilon_m^g$, typically of the order 10%. The magnitudes of the anisotropic components of $\delta\epsilon_m^{g,u}$ relative to the isotropic component of $\delta\epsilon_m^g$ are determined from the normal and parallel orientations of the molecule to the surface and are represented in Table III as expansion coefficients β_m in terms of the Legendre polynomial $P_2(\cos\theta)$. The rotational anisotropies β_m^g of

TABLE III. Calculated rotational anisotropy β_R of V_R .

ϵ_m (eV)	$k_{\parallel} (a_0^{-1})$	β_m^g	β_m^u
-4.6	0.0	0.11	-0.11
-6.2	0.0	0.15	-0.17
-6.2	0.343	0.28	-0.17

these metal states due to the interaction with the molecular ground state σ_g are consistent with the previously calculated value of $\beta_R = 0.18$. The negative sign of β_m^u can be understood from the fact that the interaction of σ_u with the metal state with parallel wave vector $k_{\parallel} = 0$ is zero by symmetry for the parallel orientation $\theta = 90^\circ$ and the gain in the interaction energy due to a symmetry allowed virtual transition into σ_u for the normal orientation $\theta = 0^\circ$. The calculated magnitude of β_m^u due to the interaction with σ_u shows that this interaction is sufficiently strong to cancel a large part of the rotational anisotropy due to the interaction with σ_g . Note that for a nonzero parallel wave vector the cancellation is less complete and suggests that the rotational coupling is stronger for processes involving phonons or exchange of reciprocal lattice vectors.

V. SUMMARY

We have measured the rotational substate splittings of corrugation mediated selective adsorption resonances observed for H_2 nozzle beams scattered from a Cu(100) surface. We assigned the rotational substates using the observed relative splittings of the states and the relative resonance intensities. Our analysis of the experimental data shows that *the rotational anisotropy is found to be dominated by the van der Waals attraction* in disagreement with results from the standard theory of physisorption which states that the repulsive part of the physisorption interaction dominates the anisotropy. We noted that the H_2 -Cu(100) and H_2 -Ag(110) systems display similar anisotropic interaction provided one accepts the experimentally suggested ordering of the substates in the latter case.

We present evidence that the standard theory of physisorption misses an important ingredient of the rotational anisotropy: the anisotropic interaction of the metal electron states with the antibonding resonance of H_2 . A simple model calculation within an extension of the theory, including this interaction term, shows that the anisotropy due to the interaction of the molecular ground state with the metal states is more or less canceled by this term. We believe that the anisotropic interaction with the antibonding resonance is the primary correction to the calculational approach, but we do not exclude that other effects may also be involved.

The new anisotropic interaction potential proposed by our analysis has important implications concerning the strength of rotational inelastic transitions. This potential has a functional behavior different from the old potential which makes the translational-rotational energy conversion inefficient. For instance, it is found to give much less strength for rotation-mediated selective adsorption reso-

nances of H₂ on Cu(100) than the old potential. This explains a puzzling observation; why no RMSA resonances were observed on this surface although the old potential gave strengths of similar magnitude as the ubiquitous CMSA resonances. The observed unexpected strength of combined resonances may be a consequence of incomplete cancellation of the rotational anisotropy for metal electron states determining the corrugation of the interaction potential.

ACKNOWLEDGMENTS

We are grateful to J. Harris for pointing out the possibility that the interaction of the metal states with the molecular antibonding state could be an important contribution to the rotational anisotropy. Financial support from the Swedish Natural Science Research Council is also gratefully acknowledged.

APPENDIX

This section presents our electronic structure model and a few technical details about the Monte Carlo evaluation of the multicenter Coulomb integrals hidden in the terms (8) and (9). In order to make close contact with the calculations by Nordlander, Holmberg, and Harris,¹⁰ we have adopted their model for the one-electron wave functions of the molecule and the metal. The calculation of the one-electron energy ϵ_u for the antibonding molecular state σ_u is also described in more detail.

First we present the Hartree-Fock model for the hydrogen molecule. The molecular ground-state wave function $\psi_g(\mathbf{x})$ is a symmetric linear combination of hydrogen 1s orbitals and the antisymmetric combination is used as a model for the wave function ψ_u of the antibonding state $|u\rangle$, and both are given in the body frame by

$$\psi_{g,u} = \frac{1}{\sqrt{2(1\pm S)N}} [\exp(-\lambda|\mathbf{x}-\mathbf{d}/2|) \pm \exp(-\lambda|\mathbf{x}+\mathbf{d}/2|)], \quad (\text{A1})$$

where \mathbf{d} is the relative position vector between the hydrogen atoms, $d=1.4a_0$, and S is the overlap of the two corresponding hydrogen 1s orbitals with normalization factor $N=\pi\lambda^{-3}$. The optimum value for λ in the wave function $\psi_g(\mathbf{x})$ is $1.189a_0$ and gives $\epsilon_g^0 = -0.595H$. Since we are only interested in an estimate of the effects of the interaction with σ_u , no separate optimization of λ has been attempted and the same value as for σ_g has been used. The one-electron energy ϵ_u of the unoccupied antibonding level is given by

$$\epsilon_\mu = \langle u | h_{\text{mol}}^{\text{HF}} | u \rangle = \left\langle u \left| -\frac{\nabla^2}{2} \right| u \right\rangle + \langle u | v_N | u \rangle + 2[uu|gg] - [ug|ug], \quad (\text{A2})$$

where $h_{\text{mol}}^{\text{HF}}$ is the Hartree-Fock Hamiltonian for the ground state of the hydrogen molecule. All these terms have been evaluated for the model wave functions (A1)

for $|g\rangle$ and $|u\rangle$ using the analytical expressions for the two-electron integrals listed in the book by Slater,¹⁸ which gives $\epsilon_u^0 = 0.607H$.

The jellium model has been used in the description of the metal and has been renormalized in the same manner as in Ref. 10 so that the observed work function $\Phi=4.59$ eV is reproduced for Cu(100). A metal state with a parallel wave vector \mathbf{k}_\parallel is approximated in the spirit of the WKB approximation as an inhomogeneous plane wave close to the molecule,

$$\psi_m(\mathbf{x}) \approx \psi_m(\mathbf{X}) \exp[i\mathbf{k}_\parallel(\mathbf{X}-\mathbf{x})] \exp[-\kappa(z-Z)]. \quad (\text{A3})$$

The decay constant κ is given by the local wave vector $\kappa = \{2[v_{\text{met}}(Z) - \epsilon_m k_\parallel^2]\}^{1/2}$ and \mathbf{X} is the position vector for the center of mass of the molecule. The amplitude $\psi_m(\mathbf{X})$ of the metal wave function at the molecule is irrelevant in our discussion since we are only interested in the relative magnitude between the anisotropic and isotropic component of the repulsion. The square of this amplitude is common both for ϵ_m^g and ϵ_m^u and their functional forms with Z are expected to be the same. In this analysis it is thus sufficient to consider the equilibrium position $Z_{\text{eq}} = 4.83a_0$ as a typical distance from the jellium edge. The metal wave function that has the slowest decay away from the surface propagates normal to the surface with an energy equal to the Fermi energy ϵ_F . However, the density of states is zero for wave functions with a normal energy $\epsilon_\perp = \epsilon_F$. A simple estimate based on the exponential decay of the wave functions in the physisorption region shows that the dominant contribution to the sum (7) comes from states with normal energies $\epsilon_F - \epsilon_\perp \approx \sqrt{[\Phi + v_{\text{met}}(Z)]/2Z} \approx 1-2$ eV at $Z = Z_{\text{eq}}$.

The Coulomb integrals—direct and exchange—appearing in $\langle m | v_{\text{mol}} | m \rangle$ and $\langle m | v_{\text{mol}} | u \rangle$ are all calculated using a Monte Carlo integration procedure. The overlap matrix element $\langle g | m \rangle$ was calculated analytically. In the Hartree-Fock approximation all the Coulomb matrix elements are given by

$$\begin{aligned} \langle m | v_{\text{mol}} | m \rangle &= \langle m | v_N | m \rangle + 2[mm|gg] - [mg|mg], \\ \langle m | v_{\text{mol}} | u \rangle &= \langle m | v_N | u \rangle + 2[mu|gg] - [mg|ug], \end{aligned} \quad (\text{A4})$$

where v_N is the electrostatic energy of an electron in the field from the nuclei and the Slater notation has been introduced for the other Coulomb integrals.¹⁸ The Metropolis algorithm has been used for generating appropriate sampling distributions. The trial steps are taken with maximum step size of $1.0a_0$. The correlations in this random walk have been controlled in a standard manner by calculating the autocorrelation function. A sampling interval of 40 steps was sufficient to make the autocorrelations less than 0.1. Typically, about 40 000 and 160 000 samples for the direct and exchange integrals, respectively, were used to get an estimated relative variance of 10–20% for the final results for β_m in Table III.

The large cancellation between the matrix elements due to the direct Coulomb interaction of the metal electron with the molecular nuclear charge and the electron density of the molecular ground state, respectively, in

Eqs. (A4) requires some care in the Monte Carlo procedure. This cancellation has been reduced by approximating the ground-state density by a model density comprising three $1s$ densities with the same decay constants as used in the model for the ground state in Eq. (A1): one centered around each nuclei and one at the midcenter of the molecule. Their individual strengths have been adjusted so that the total number of electrons and the quadrupole moment of the molecule is reproduced. The virtue of this model density is that its electrostatic potential can be calculated analytically. The deviation of this model density from the true density as determined from Eq. (A1) is then handled by the Monte Carlo integration procedure. In this case a $1s$ wave function

centered at the midcenter with the same decay constants as for the $1s$ functions in the molecular ground state, Eq. (A1), has been used as a sampling function.

When calculating the exchange integrals, some precautions are also needed in the choice of the sampling function in order to have a sensible estimate of the variance. The exponential increase of the metal wave function $\psi_m(\mathbf{x})$, Eq. (A3), towards the metal, makes the variance divergent for the molecular ground-state wave function $\psi_g(\mathbf{x})$, Eq. (A1), as a sampling function, since $2\mu > \lambda_g$. This divergence is avoided by first multiplying $\psi_g(\mathbf{x})$ with an exponentially increasing radial function centered at the midcenter of the molecule with a growth constant μ , since $\mu < \lambda_g$ for the metal wave functions.

-
- ¹M. R. Hand and S. Holloway, *J. Chem. Phys.* **91**, 7209 (1989).
²J. Harris, *Surf. Sci.* **221**, 335 (1989).
³B. E. Hayden and C. R. A. Lamont, *Phys. Rev. Lett.* **63**, 1823 (1989).
⁴J. Lapujoulade, *Surf. Sci.* **108**, 526 (1981).
⁵C.-F. Yu, K. B. Whaley, C. S. Hogg, and S. J. Sibener, *Phys. Rev. Lett.* **51**, 2210 (1983); *J. Chem. Phys.* **83**, 4217 (1985).
⁶S. Andersson, L. Wilzén, M. Persson, and J. Harris, *Phys. Rev. B* **40**, 8146 (1989).
⁷M. Chiesa, L. Mattera, R. Musenich, and C. Salvo, *Surf. Sci.* **151**, L145 (1985).
⁸R. Schinke, V. Engel, and H. Voges, *Chem. Phys. Lett.* **104**, 279 (1984).
⁹J. Harris and P. J. Feibelman, *Surf. Sci.* **115**, 133 (1982).
¹⁰P. Nordlander, C. Holmberg, and J. Harris, *Surf. Sci.* **152**, 702 (1985).
¹¹A recent simplified calculation of the repulsive part based on a semiempirical electron-gas model gave as a result a total potential that favors rotations around an axis parallel to the surface. The anisotropy of the attractive part of this potential is also given by $\beta_{vw}V_{vw}(z)$ with $\beta_{vw}=0.06$ [G. Ihm and M. W. Cole, *Langmuir* **5**, 550 (1989)].
¹²K. B. Whaley, C. Yu, C. S. Hogg, J. C. Light, and S. Sibener, *J. Chem. Phys.* **83**, 4235 (1985).
¹³S. Andersson, L. Wilzén, and M. Persson, *Phys. Rev. B* **38**, 2967 (1988).
¹⁴The importance of hybridization interactions in physisorption has been stressed by Anett and Haydock for the interaction of He with metal surfaces [J. F. Anett and R. Haydock, *Phys. Rev. Lett.* **53**, 838 (1984); *Phys. Rev. B* **34**, 6860 (1986). Their interaction term is qualitatively different from our inter-polarization term and derives from the interaction of the He $1s$ orbital with the unoccupied metal states. The magnitude of their hybridization term is still controversial [J. Harris and E. Zaremba, *Phys. Rev. Lett.* **55**, 1940 (1985)].
¹⁵E. Zaremba and W. Kohn, *Phys. Rev. B* **15**, 1769 (1977).
¹⁶J. Harris, *Phys. Rev. B* **31**, 1770 (1985).
¹⁷J. Harris and A. Liebsch, *J. Phys. C* **15**, 2275 (1982).
¹⁸J. C. Slater, *Quantum Theory of Molecules and Solids* (McGraw-Hill, New York, 1960), Vol. 1.